

Thermoelectric model to characterize carrier transport in organic semiconductors

Gunho Kim¹ and Kevin P. Pipe^{1,2,*}

¹*Department of Mechanical Engineering, University of Michigan, Ann Arbor, Michigan 48109-2125, USA*

²*Department of Electrical Engineering and Computer Science, University of Michigan, Ann Arbor, Michigan 48109-2122, USA*

(Received 8 March 2012; revised manuscript received 15 August 2012; published 29 August 2012)

A model for the Seebeck coefficient in the regime of hopping transport that includes the effects of Gaussian carrier density of states width and carrier localization allows these parameters to be derived independently of the attempt-to-jump rate, which can subsequently be derived from measured electrical conductivity. This model is applied to prototypical small molecular and polymer organic semiconductors to characterize carrier localization, quantify the role of dopants on the hopping transport parameters, and derive the effective dopant ionization fraction and activation energy.

DOI: [10.1103/PhysRevB.86.085208](https://doi.org/10.1103/PhysRevB.86.085208)

PACS number(s): 72.80.Le, 63.20.kd, 72.20.Ee, 72.20.Pa

I. INTRODUCTION

Carrier transport in organic semiconductors (OSCs) has traditionally been described by a thermally activated hopping process between localized states that have an energetic disorder modeled by a Gaussian distribution.¹⁻³ In this description, three material properties dictate carrier mobility (μ): the carrier localization length (α) relative to the distance between hopping sites; the intrinsic attempt-to-jump rate (v_0), which depends on the strength of electron-phonon coupling and phonon density of states; and the degree of energetic disorder, as quantified by the standard deviation (a_{DOS}) of the carrier density of states (DOS). Since all three parameters directly influence mobility, it has proven difficult to derive independent values for them from fits to measured electrical conductivity (σ) or mobility. This has led to broad quantitative uncertainty (for example, reported values⁴⁻⁸ of v_0 vary by more than seven orders of magnitude depending on what values are assumed for the other parameters) and broad qualitative uncertainty (in particular, the effect of molecular structure on mobile carrier localization) regarding the nature of charge transport in OSCs. Inconsistencies further exist between models and experiments; for example, models⁵⁻⁷ traditionally assume α to be much less than the molecular spacing (l) and fit data for high-mobility OSCs using very large values of v_0 ,^{6,7} yet these assumptions are inconsistent with measurements showing the mobility to have a flat or negative temperature dependence^{9,10} and the carrier wave function to have a size greater than l ,¹¹ both of which have been interpreted as indicative of “bandlike” transport.^{10,11} Furthermore, as OSCs become increasingly utilized for device applications¹²⁻¹⁵ it is critical to quantitatively assess the effects of dopants on carrier localization and other hopping parameters.

Because the Seebeck coefficient (S) is related to the average energy of conducting carriers, it is sensitive to the DOS shape (e.g., a_{DOS}) and the wave-function overlap for carriers of a particular energy (e.g., α). It is not, however, sensitive to v_0 under the normal assumptions of thermally activated hopping,^{2,16} for which this rate is energy independent.

Here we present a model for S and σ in the case of a Gaussian DOS that provides their explicit analytic dependences on a_{DOS} and α . We then use this model to derive a_{DOS} , α , and v_0 for the prototypical high-mobility small molecular OSC pentacene and the prototypical high-mobility polymer OSC

poly(3,4-ethylenedioxythiophene) (PEDOT). This method indicates $\alpha > l$ for both materials, which the model further shows to be consistent with a very weak (bandlike) dependence of mobility on temperature. We then show how bulk doping and a field-effect geometry impact the hopping parameters of pentacene differently, and analyze the impact of additives and dopant type on the hopping parameters of PEDOT.

II. MODEL

S is proportional to the average energy of conducting charge carriers with respect to the Fermi energy (E_F):

$$S = -\frac{k}{q} \int_{-\infty}^{\infty} \frac{(E - E_F) \sigma(E)}{kT \sigma} dE = -\frac{1}{qT} (E_{\text{tr}} - E_F), \quad (1)$$

where k and q are the Boltzmann constant and unit charge. To facilitate comparison with crystalline inorganic solids, we define the transport energy as the mean energy of conducting charge carriers:

$$E_{\text{tr}} = \frac{1}{\sigma} \int_{-\infty}^{\infty} E \sigma(E) dE, \quad (2)$$

rather than the energy at which the hopping rate is fastest.⁷ In the weak field limit, the Miller-Abrahams hopping model gives the transition rate between sites i and j as¹

$$v_{ij} = v_0 \exp \left[-2 \frac{R_{ij}}{\alpha} - \frac{E_j - E_i}{kT} \theta(E_j - E_i) \right], \quad (3)$$

where R_{ij} is the intersite distance, E_i is the energy at site i , and $\theta(E_j - E_i)$ is the Heaviside unit step function. This model has been shown to agree well with experimental data on OSCs, including those with high carrier concentrations.^{4,17} The average rate $v(E)$ at which carriers transition from energy E to a different energy (i.e., the escape rate) is given by the sum of the average downward [$v_{\downarrow}(E)$] and upward [$v_{\uparrow}(E)$] hopping rates:

$$v_{\downarrow}(E) = v_0 \exp \left[-2 \frac{R(E)}{\alpha} \right], \quad (4a)$$

$$\begin{aligned} v_{\uparrow}(E) &= \int_E^{\infty} \exp \left(-\frac{\varepsilon - E}{kT} \right) v_{\downarrow}(\varepsilon) h(\varepsilon) d\varepsilon, h(\varepsilon) \\ &= \frac{g(\varepsilon) [1 - f(\varepsilon)]}{\int_E^{\infty} g(\varepsilon) [1 - f(\varepsilon)] d\varepsilon}, \end{aligned} \quad (4b)$$

where $g(\varepsilon)$ is the carrier DOS, $f(\varepsilon)$ is the Fermi-Dirac distribution, and the average distance carriers at energy E must hop is given by⁷

$$R(E) = \left\{ \frac{4\pi}{3B} \int_{-\infty}^E g(\varepsilon) [1 - f(\varepsilon)] d\varepsilon \right\}^{-1/3}, \quad (5)$$

which takes into account state filling at high carrier concentrations as well as the percolation threshold parameter B (~ 2.7).¹⁸ In contrast to other hopping models,^{5-8,16} the formulation of Eqs. (4) and (5) allows straightforward calculation of the energy-dependent hopping rate $v(E)$, which is essential for evaluation of S . While the DOS for inorganic semiconductors (ISCs) with static disorder is typically represented by a parabolic band of extended states with a small percentage of localized states occupying an exponential tail,¹⁹ the DOS for OSCs is primarily made up of localized states (due to the sensitivity of weak bonds to dynamic disorder²⁰) and is typically Gaussian:^{3,21,22}

$$g(\varepsilon) = \frac{N_t(n_d)}{\sqrt{2\pi a_{\text{DOS}}^2}} \exp\left(-\frac{\varepsilon^2}{2a_{\text{DOS}}^2}\right), \quad (6)$$

where a_{DOS} depends on material morphology.²³ To approximate the effect of dopant volume, which increases hopping distance and thereby exponentially decreases the transition rate, we introduce a total DOS N_t that depends on the dopant concentration (n_d):

$$N_t(n_d) = \frac{N_0}{1 + rn_d/N_0} = \eta(r, n_d)N_0, \quad (7)$$

where r is the ratio between the dopant and host molecule volumes and N_0 is the intrinsic (undoped) DOS, assumed equal to the intrinsic molecular density.²⁴ The carrier mobility can be calculated using the generalized Einstein relation (valid to high carrier concentrations).^{25,26}

$$\mu(E) = \frac{q}{kT} [1 - f(E)] \left[R(E)^2 v_{\downarrow}(E) + \int_E^{\infty} R(\varepsilon)^2 \exp\left(-\frac{\varepsilon - E}{kT}\right) v_{\downarrow}(\varepsilon) h(\varepsilon) d\varepsilon \right]. \quad (8)$$

The carrier concentration-dependent mobility $\mu(n)$ can then be written in terms of the energy-dependent conductivity $\sigma(E) = qg(E)f(E)\mu(E)$ as

$$\mu(n) = \eta^{1/3} \exp\left[2\frac{l(1 - \eta^{-1/3})}{\alpha}\right] \left[\frac{\int_{-\infty}^{\infty} \sigma(E) dE}{qn} \right]_{r=0}, \quad (9)$$

where l is the molecular spacing and the free carrier concentration n is given by

$$n = bn_d = \int_{-\infty}^{\infty} g(\varepsilon) f(\varepsilon) d\varepsilon, \quad (10)$$

where b is the effective ionization fraction defined as the number of mobile carriers per dopant. At low carrier concentrations, semianalytic expressions can be derived for σ and S . The conductivity and mobility [valid for $(l/\alpha)^3 \gg 1$, $n/N_0 < 10^{-2}$] are given by

$$\sigma = qn\mu = qn\mu_0 \exp\left[-p_0 - C_1 \hat{a}_{\text{DOS}} - \left(C_2 - \frac{C_3}{p_0}\right) \hat{a}_{\text{DOS}}^2\right] \exp\left[\frac{1}{2} (\hat{a}_{\text{DOS}}^2 - \hat{a}_{\text{DOS}}) \left(\frac{2n}{N_t}\right)^{\delta}\right], \quad (11)$$

where $\mu_0 = ql^2 v_0 / a_{\text{DOS}}$, $\hat{a}_{\text{DOS}} = a_{\text{DOS}} / kT$, $p_0 = C_4 (B / N_t \alpha^3)^{1/3}$, and $\delta = (2 / \hat{a}_{\text{DOS}}^2) [\ln(\hat{a}_{\text{DOS}}^2 - \hat{a}_{\text{DOS}}) - \ln(\ln 4)]$. Constants C_1 , C_2 , C_3 , and C_4 have best-fit values of 0.26, 0.51, 1, and 1.44, respectively; this four-constant parametrization and the associated numerical values are consistent with OSCs under a range of transport models.⁵ The Seebeck coefficient (valid for $n/N_t \ll 10^{-6}$) is given by

$$S = \frac{E_F - E_{tr}}{qT} = \frac{1}{qT} \left(\left(kT \ln \frac{n}{N_t} - \frac{1}{2} \frac{a_{\text{DOS}}^2}{kT} \right) - \left\{ \frac{a_{\text{DOS}}}{4} \left[\ln \left(\sqrt{\frac{2}{\pi}} \frac{2B}{9\pi^2} \right) - \frac{7}{5} \sqrt{\hat{a}_{\text{DOS}}} \ln \hat{a}_{\text{DOS}} + \ln \frac{1}{N_t \alpha^3} \right] \right\} \right). \quad (12)$$

Numerical calculations can be used to examine transport at relatively large delocalization ($\alpha > l$) or high carrier concentrations. Figure 1(b) plots normalized mobility (μ/μ_0) calculated using (9) versus normalized carrier concentration (n/N_0) for two values of r and several values of a_{DOS} that are typical of OSCs at room temperature. Also shown in Fig. 1(b) are the results of a numerical solution of the master equation for hopping transport⁶ that does not use the averaging approximations of Eqs. (4) and (5). Since the master equation approach assumes that hopping primarily occurs between nearest neighbors, $R(E_{tr})$ is set equal to l and incorporated into the general equations (9) and (11) for this figure, a method previously utilized⁷ to facilitate comparisons of other models with the master equation approach. Good agreement is found up to a normalized carrier concentration of 10^{-2} , beyond

which the mobility is known to decrease as predicted by the model developed here due to the occupation probability of final states.⁵ Comparison of the two models supports the use of Eqs. (4) and (5) to derive the energy-dependent hopping rate $v(E)$.

It is apparent from Fig. 1(c) that $dS/d(\ln n)$ is primarily governed by a_{DOS} and relatively unaffected by α . Given data for $S(n)$, therefore, a_{DOS} can first be determined by a slope fit and α can then be determined by a subsequent fit. With these two parameters, v_0 can then be determined by a fit to σ data.

III. COMPARISON WITH EXPERIMENTAL DATA

To demonstrate this independent fitting of the three hopping parameters, Fig. 2(a) shows experimental data for a pentacene

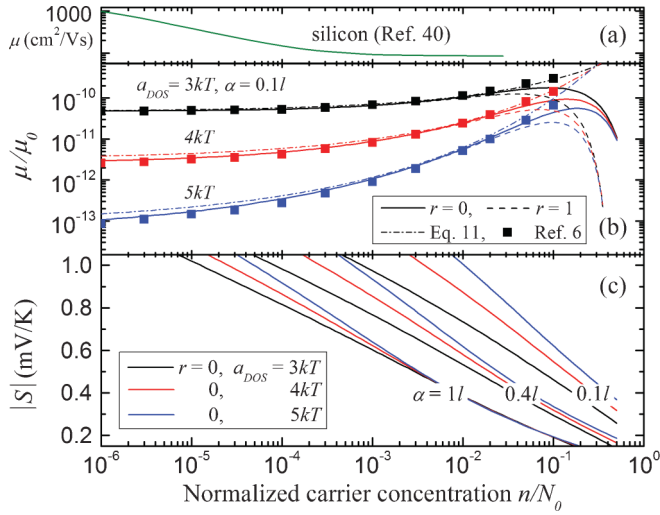


FIG. 1. (Color online) (a) Electron mobility in silicon at $T = 300$ K (Ref. 40). N_0 for Si is set as its atomic density ($5 \times 10^{22} \text{ cm}^{-3}$). (b) OSC mobility at 300 K as calculated by Eq. (9) (solid and dashed lines) and a master equation for hopping transport (Ref. 6) (symbols). $\alpha = 0.1l$ is used for both and b is set to unity. Also shown is the low carrier concentration expression of Eq. (11) (dot-dashed lines). (c) Calculation of $|S|$.

field-effect transistor (FET)¹⁰ and a 2,3,5,6-tetrafluoro-7,7,8,8-tetracyanoquinodimethane ($\text{F}_4\text{-TCNQ}$) doped bulk pentacene film²⁷ at room temperature. By a slope fit, we find $a_{\text{DOS}} =$

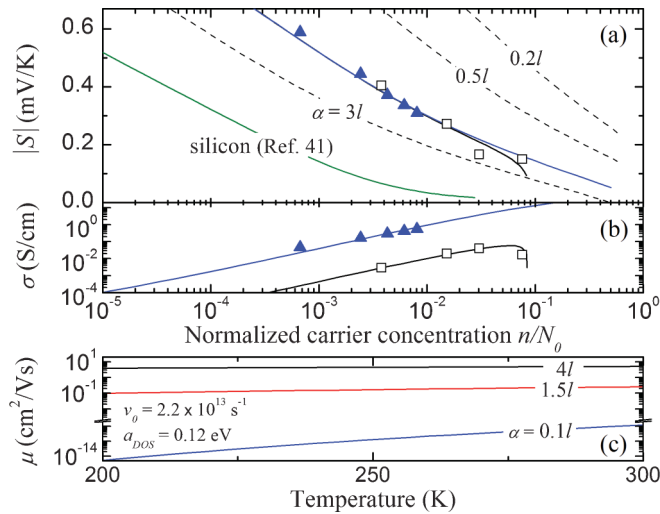


FIG. 2. (Color online) (a) and (b) Calculated S and σ for various α . Measured room temperature data for pentacene FETs (Ref. 10) (closed symbols), doped bulk pentacene films (Ref. 27) (open symbols), and silicon (Ref. 41) are also shown. $N_0 = 2.9 \times 10^{21} \text{ cm}^{-3}$ is used for pentacene (Ref. 24). Measured FET channel densities are converted to carrier concentrations based on the effective FET channel thickness (3 nm) (Ref. 28). Measured dopant mole fractions for the bulk film are converted to carrier concentrations based on $b = 0.76$ as reported for $\text{F}_4\text{-TCNQ}$ in pentacene (Ref. 27). Measured field-effect mobility is used to calculate σ for the FET, since it is typically similar to the Hall mobility for small molecular FETs (Refs. 10 and 29). (c) Temperature dependence of mobility for several values of α at $n/N_0 = 10^{-2}$, a typical concentration for operating FETs.

0.12 eV for both the FET and the bulk film; using this, we then derive $\alpha = 1.5l$ for both. Using these values, we then derive $v_0 = 2.2 \times 10^{13} \text{ s}^{-1}$ for the FET and $2.5 \times 10^{11} \text{ s}^{-1}$ for the bulk film [Fig. 2(b)]. For the bulk film, fitting σ at high n allows $r = 8$ to be derived (which is a reasonable volume expansion for impurities in pentacene³⁰), while $r = 0$ for the FET since no dopants are present.

The derived α suggests more than an order of magnitude greater delocalization of carriers in pentacene than that typically assumed for OSCs in hopping models.⁵⁻⁷ This delocalization results in a predicted temperature dependence of mobility that is very weak based on our model [Fig. 2(c)], whereas mobility follows a $\ln(\mu) \sim -1/T$ relationship for strongly localized carriers [$(l/\alpha)^3 \gg 1$] at vanishing carrier concentrations. These model predictions are consistent with prior measurements of polycrystalline pentacene FETs¹⁰ which found that field-induced carriers are not fully extended but instead localized with a length larger than the molecular spacing, even though the mobility demonstrates a bandlike temperature dependence. Furthermore, the derived hopping parameters suggest that ionized dopants in pentacene primarily affect electron-phonon coupling and the phonon DOS rather than carrier localization. The wave functions of mobile carriers remain governed by the host molecules between which hopping takes place³¹ (consistent with measurements of polyaniline in which α was found to remain nearly constant regardless of the dopant used³²), while volume expansion or other conformational changes due to dopant incorporation soften the material, reducing its elastic modulus³³ and redshifting the dominant phonon frequency³⁴ at which electron coupling occurs. The much larger value of v_0 for the FET is also consistent with its much larger mobility ($0.15 \text{ cm}^2/\text{Vs}$)¹⁰ compared to $\text{F}_4\text{-TCNQ}$ doped bulk pentacene (0.0016 to $0.0028 \text{ cm}^2/\text{Vs}$).²⁷

We note that if hopping transport occurs in an OSC for which complexities such as carrier percolation along grain boundaries exist, the derived hopping parameters will represent effective values which depend to some extent on film morphology; for example, samples with smaller grain size and hence larger disorder may be expected to have a larger DOS width.²³ However, an isotropic hopping model with a regular cubic lattice such as the one assumed here has successfully described transport in many small molecular^{23,35} and conjugated polymer⁴⁻⁶ OSCs.

Dopant type is known to have a strong effect on transport in PEDOT, as evidenced by recent observations in which the maximum thermoelectric power factor ($S^2\sigma$) was found to increase from $6.0 \times 10^{-6} \text{ W/mK}^2$ when doped with poly(styrenesulfonate) (Pss)³⁶ to $3.24 \times 10^{-4} \text{ W/mK}^2$ when doped with tosylate (Tos) [Fig. 3(a)],¹⁵ raising the thermoelectric figure of merit from 0.01 to 0.25. Literature studies of S in PEDOT and other polymer OSCs typically do not measure free carrier concentration directly but instead measure oxidation level ($\text{ox} = n_d/N_t$), which gives the fraction of ionized dopants. However, not all ionized dopants contribute mobile carriers,³¹ resulting in an effective ionization fraction (b) less than unity:³⁷

$$\frac{n}{n_d} = b = \exp(-E_a/kT) = \exp[-(E_{a,\text{max}} - \beta n_d^{1/3})/kT], \quad (13)$$

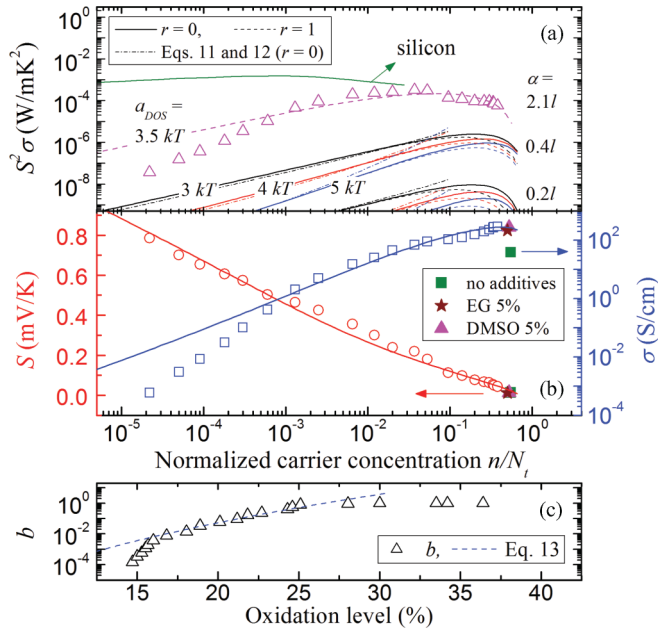


FIG. 3. (Color online) (a) Room temperature $S^2\sigma$ measured (Ref. 15) in PEDOT:Tos (symbols) and calculated for a general OSC and silicon (lines) (Refs. 40 and 41). The value of v_0 derived for PEDOT:Tos ($1 \times 10^{14} \text{ s}^{-1}$) for $\text{ox} > 16\%$ is assumed in general OSC calculations. (b) S and σ vs n/N_t for PEDOT:Tos (Ref. 15) (open symbols) and PEDOT:Pss (Ref. 36) (closed symbols). $N_t = 10^{21} \text{ cm}^{-3}$ and $r \sim 1$ (based on molecular weights of Tos and EDOT) are used for numerical calculations (Ref. 39). (c) Effective ionization fraction calculated for PEDOT:Tos (symbols) and a fit to Eq. (13) (dashed line).

where $E_{a,\text{max}}$ is the maximum activation energy of the dopant at dilute concentrations and β captures the dependence of E_a on dopant concentration. To convert oxidation level to n for PEDOT:Tos,¹⁵ we first note that $dS/d(\ln \text{ox})$ for low oxidation levels ($< 25\%$) is much greater in magnitude than the characteristic value of $-k/q$, implying that b is increasing. For high oxidation levels ($> 25\%$), $dS/d(\ln \text{ox})$ is very close to $-k/q$, implying that b is constant; we take this constant to be unity (i.e., each additional ionized dopant contributes one mobile carrier). While this high-concentration region provides a sufficient basis on which to derive the hopping parameters, the sensitivity of S to free carrier concentration further enables derivation of b , β , and $E_{a,\text{max}}$. By simultaneously fitting the measured S and σ data for $\text{ox} > 16\%$ using the S and σ models developed above as well as Eq. (13), we find $E_{a,\text{max}} = 0.83 \text{ eV}$, which is on the order of the exciton binding energy in OSCs,³⁸ and $\beta = 1.3 \times 10^{-7} \text{ eV cm}$, which is similar to its value in other OSCs.³⁷ Below 16% oxidation level, b changes rapidly, which we attribute to the strong binding energy of the accumulated tetrakis(dimethylamino)ethylene (TDAE) species used to dedope the PEDOT:Tos. For these five lowest-concentration data points, the effect of the TDAE is apparent in σ but not S , suggesting that v_0 is reduced while α is unaffected, as with F₄-TCNQ in pentacene.

A fit to $dS/d(\ln n)$ yields $a_{\text{DOS}} = 3.5 \pm 0.4kT$, which is typical for PEDOT.⁸ Fits to S vs n and σ vs n yield $\alpha = 2.1l$ and $v_0 = 1 \pm 0.2 \times 10^{14} \text{ s}^{-1}$, respectively, for PEDOT:Tos. As shown in Fig. 3(a), data for PEDOT:Tos, PEDOT:Pss

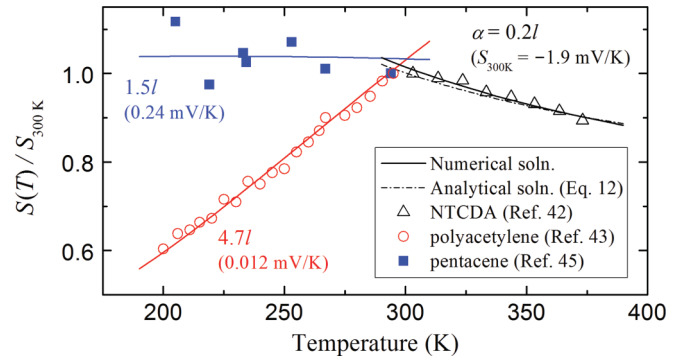


FIG. 4. (Color online) Fits of the model to further experimental data, demonstrating how $d|S|/dT$ changes as α increases from an activated ($|S| \sim 1/T$) regime in NTCDA to an intermediate ($|S| \sim \text{const.}$) regime in pentacene to a VRH ($|S| \sim T$) regime in polyacetylene.

without additives, PEDOT:Pss with 5% ethylene glycol (EG), and PEDOT:Pss with 5% dimethyl sulfoxide (DMSO)³⁶ all fall on the same S curve, indicating that α is unaffected by dopants or additives. However, as is clear from the plot of σ , v_0 in PEDOT:Pss increases considerably in the presence of additives (no additives: $1.4 \pm 0.2 \times 10^{13}$, EG: $7.9 \pm 0.2 \times 10^{13}$, DMSO: $1 \pm 0.2 \times 10^{14} \text{ s}^{-1}$), consistent with the fact that DMSO and EG are known to produce rodlike conformations that increase the polymer's elastic modulus.³³ As with pentacene, these results suggest that the primary effect of doping in PEDOT is on its vibronic characteristics, which impact the intrinsic attempt-to-jump rate v_0 ; the enhancement of maximum $S^2\sigma$ in PEDOT:Tos vs PEDOT:Pss is due to an increase in electron-phonon coupling or change in the phonon DOS rather than an increase in carrier delocalization. This maximum $S^2\sigma$ occurs at a high carrier concentration (as predicted by our model) as the distribution of conducting carriers shifts to high energies where μ is much larger. It should be noted that additional scattering mechanisms (e.g., impurity scattering) will affect carrier localization and transport for large values of α ($\alpha \gg l$).

We can likewise characterize transport in OSCs by examining fits to S vs T (Fig. 4). For Naphthalenetetracarboxylic dianhydride (NTCDA), a fit of the model to experimental data⁴² yields $\alpha = 0.2l$ and $n/N_t = 5.2 \times 10^{-7}$. Both the numerical (Fermi-Dirac) and analytical [Eqs. (11) and (12)] solutions for σ (not shown) and S are accurate in this highly localized, low carrier concentration regime, in which both properties are expected to exhibit an activation energy.¹⁹ Consistent with this expectation, σ and S both show an activated ($\sim 1/T$) temperature dependence. The activation energies derived by the model for the values of α and n/N_t given above are $\varepsilon_{a,\sigma} = 404 \text{ meV}$ and $\varepsilon_{a,S} = 326 \text{ meV}$, which are very close to the measured values⁴² of $\varepsilon_{a,\sigma} = 400 \text{ meV}$ and $\varepsilon_{a,S} = 330 \text{ meV}$. For polyacetylene, a fit of the model to experimental data⁴³ yields $\alpha = 4.7l$ and $n/N_t = 2.34 \times 10^{-1}$; this relatively delocalized, high carrier concentration regime is consistent with variable-range hopping (VRH) transport. The model accurately shows that S increases with T (consistent with VRH¹⁹) and that the increase is approximately linear (similar to the predicted temperature dependence of VRH for

an exponential DOS⁴⁴). Finally, we show $S(T)$ predicted by the model for pentacene at $n/N_t = 2.1 \times 10^{-2}$, where we have used the localization length ($\alpha = 1.5 l$) derived above from fits to S vs n . While the available S vs T data for a pentacene FET⁴⁵ are somewhat noisy, they do appear to follow the predicted trend.

ACKNOWLEDGMENTS

This work was supported as part of the Center for Solar and Thermal Energy Conversion, an Energy Frontier Research Center funded by the US Department of Energy Office of Science, Office of Basic Energy Sciences under Award No. DE-SC0000957.

*pipe@umich.edu

- ¹A. Miller and E. Abrahams, *Phys. Rev.* **120**, 745 (1960).
- ²H. Bässler, *Phys. Status Solidi B* **175**, 15 (1993).
- ³I. N. Hulea, H. B. Brom, A. J. Houtepen, D. Vanmaelbergh, J. J. Kelly, and E. A. Meulenkaamp, *Phys. Rev. Lett.* **93**, 166601 (2004).
- ⁴V. I. Arkhipov, P. Heremans, E. V. Emelianova, G. J. Adriaenssens, and H. Bässler, *Appl. Phys. Lett.* **82**, 3245 (2003).
- ⁵R. Coehoorn, W. F. Pasveer, P. A. Bobbert, and M. A. J. Michels, *Phys. Rev. B* **72**, 155206 (2005).
- ⁶W. F. Pasveer, J. Cottaar, C. Tanase, R. Coehoorn, P. A. Bobbert, P. W. M. Blom, D. M. de Leeuw, and M. A. J. Michels, *Phys. Rev. Lett.* **94**, 206601 (2005).
- ⁷I. I. Fishchuk, V. I. Arkhipov, A. Kadashchuk, P. Heremans, and H. Bässler, *Phys. Rev. B* **76**, 045210 (2007).
- ⁸Y. Roichman, Y. Preezant, and N. Tessler, *Phys. Status Solidi A* **201**, 1246 (2004).
- ⁹T. Sakanoue and H. Sirringhaus, *Nat. Mater.* **9**, 736 (2010).
- ¹⁰K. P. Pernstich, B. Rössner, and B. Batlogg, *Nat. Mater.* **7**, 321 (2008).
- ¹¹K. Marumoto, S. I. Kuroda, T. Takenobu, and Y. Iwasa, *Phys. Rev. Lett.* **97**, 256603 (2006).
- ¹²H. Yan, Z. Chen, Y. Zheng, C. Newman, J. R. Quinn, F. Dötz, M. Kastler, and A. Facchetti, *Nature* **457**, 679 (2009).
- ¹³S. Reineke, F. Lindner, G. Schwartz, N. Seidler, K. Walzer, B. Lüssem, and K. Leo, *Nature* **459**, 234 (2009).
- ¹⁴Y. Liang, Z. Xu, J. Xia, S. Tsai, Y. Wu, G. Li, C. Ray, and L. Yu, *Adv. Mater.* **22**, E135 (2010).
- ¹⁵O. Bubnova, Z. U. Khan, A. Malti, S. Braun, M. Fahlman, M. Berggren, and X. Crispin, *Nat. Mater.* **10**, 429 (2011).
- ¹⁶V. Ambegaokar, B. I. Halperin, and J. S. Langer, *Phys. Rev. B* **4**, 2612 (1971).
- ¹⁷C. Tanase, E. J. Meijer, P. W. M. Blom, and D. M. de Leeuw, *Phys. Rev. Lett.* **91**, 216601 (2003).
- ¹⁸B. I. Shklovskii and A. L. Efros, *Electronic Properties of Doped Semiconductors* (Springer, New York, 1984).
- ¹⁹N. F. Mott and E. A. Davis, *Electronic Processes in Non-Crystalline Materials* (Clarendon, Oxford, 1971).
- ²⁰J. Böhlín, M. Linares, and S. Stafström, *Phys. Rev. B* **83**, 085209 (2011).
- ²¹S. Yogeve, E. Halpern, R. Matsubara, M. Nakamura, and Y. Rosenwaks, *Phys. Rev. B* **84**, 165124 (2011).
- ²²R. Hesse, W. Hofberger, and H. Bässler, *Chem. Phys.* **49**, 201 (1980).
- ²³M. Ullah, I. I. Fishchuk, A. Kadashchuk, P. Stadler, A. Pivrikas, C. Simbrunner, V. N. Poroshin, N. S. Sariciftci, and H. Sitter, *Appl. Phys. Lett.* **96**, 213306 (2010).
- ²⁴D. V. Lang, X. Chi, T. Siegrist, A. M. Sergent, and A. P. Ramirez, *Phys. Rev. Lett.* **93**, 086802 (2004).
- ²⁵Y. Roichman and N. Tessler, *Appl. Phys. Lett.* **80**, 1948 (2002).
- ²⁶R. Schmechel, *J. Appl. Phys.* **93**, 4653 (2003).
- ²⁷K. Harada, M. Sumino, C. Adachi, S. Tanaka, and K. Miyazaki, *Appl. Phys. Lett.* **96**, 253304 (2010).
- ²⁸N. Yoneya, M. Noda, N. Hirai, K. Nomoto, M. Wada, and J. Kasahara, *Appl. Phys. Lett.* **85**, 4663 (2004).
- ²⁹V. Podzorov, E. Menard, J. A. Rogers, and M. E. Gershenson, *Phys. Rev. Lett.* **95**, 226601 (2005).
- ³⁰D. Käfer, Ph.D. thesis, Ruhr-Universität Bochum, Germany, 2008.
- ³¹K. Walzer, B. Maennig, M. Pfeiffer, and K. Leo, *Chem. Rev.* **107**, 1233 (2007).
- ³²P. K. Kahol, K. K. Satheesh Kumar, S. Geetha, and D. C. Trivedi, *Synth. Met.* **139**, 191 (2003).
- ³³T. E. Fisher, P. E. Marszalek, A. F. Oberhauser, M. Carrion-Vazquez, and J. M. Fernandez, *J. Physiol.* **520**, 5 (1999).
- ³⁴D. D. Dlott, *Annu. Rev. Phys. Chem.* **37**, 157 (1986).
- ³⁵Y. Hong, F. Yan, P. Migliorato, S. H. Han, and J. Jang, *Thin Solid Films* **515**, 4032 (2007).
- ³⁶C. Liu, B. Lu, J. Yan, J. Xu, R. Yue, Z. Zhu, S. Zhou, X. Hu, Z. Zhang, and P. Chen, *Synth. Met.* **160**, 2481 (2010).
- ³⁷B. A. Gregg, S. Chen, and R. A. Cormier, *Chem. Mater.* **16**, 4586 (2004).
- ³⁸M. Knupfer, *Appl. Phys. A* **77**, 623 (2003).
- ³⁹S. Kirchmeyer, A. Elschner, K. Reuter, W. Lövenich, and U. Merker, *PEDOT: Principles and Applications of an Intrinsically Conductive Polymer* (Taylor & Francis Group, Boca Raton, FL, 2011).
- ⁴⁰C. Jacoboni, C. Canali, G. Ottaviani, and A. A. Quaranta, *Solid State Electron.* **20**, 77 (1977).
- ⁴¹A. F. Ioffe, *Semiconductor Thermoelements and Thermoelectric Cooling* (Infosearch, London, 1957).
- ⁴²A. Nollau, M. Pfeiffer, T. Fritz, and K. Leo, *J. Appl. Phys.* **87**, 4340 (2000).
- ⁴³Y. W. Park, *Synth. Met.* **45**, 173 (1991).
- ⁴⁴B. Movaghar and W. Schirmacher, *J. Phys. C* **14**, 859 (1981).
- ⁴⁵A. vonMuhlenen, N. Errien, M. Schaer, M. N. Bussac, and L. Zuppiroli, *Phys. Rev. B* **75**, 115338 (2007).